# Tests on the Ductility of Asymmetric Part-through Center Cracks in Plates

by G.A. Kardomateas

ABSTRACT—Welds, shoulders or other asymmetries may eliminate one of the shear bands of symmetrically cracked parts, giving less ductility than the corresponding symmetric specimens and increasing the stiffness requirements for stability. Experiments on part-through center cracks in plates of 1018 cold finished steel show that the growth displacement in the asymmetric case is about half that of the symmetric one. Unconstrained plane strain singly grooved asymmetric tests of the same material show less ductility by a factor of two to three. Expressions for the J integral and the tearing modulus in both the asymmetric and symmetric cases are found and used to describe the growth resistance. To further understand the deformation, a macromechanical model represented by sliding off and fracture, based on an idealization of the underlying physical mechanisms, is applied to the test data.

## Introduction

The strain field for the usual symmetric crack under tension is characterized by two shear zones which, in the nonhardening case, narrow into two slip lines at $\pm 45$ deg. Asymmetric configurations may arise due to the presence of weld beads or shoulders (Fig. 1). In such cases one of the shear zones (Fig. 2) is suppressed. A fatigue crack or some other defect will tend to advance near the remaining active shear band. A study on unconstrained singly grooved plane strain fully plastic specimens[1] gave a reduced ductility in the asymmetric case, especially with less hardening. A method for quantifying and representing the ductility was also suggested.[1]

Near the tip of the growing crack, strain hardening will cause the deformation field to fan out. A shear band

characterization of mixed mode I and II fully plastic crack growth by combined fracture on one plane and sliding off along two others (simulating the finite-width effect of the shear zone) gave a description of ductile crack growth for both the asymmetric and symmetric configurations.[2]

In general, nonhardening rigid-plastic-flow fields have shown that with an asymmetric configuration there may be discontinuities in the displacements across the rigid-elastic boundary.[3] The strain concentrations may be correspondingly higher, promoting fracture. One thus would like to ensure that the ductility of the material which one would expect from usual tests is actually available. It is the objective of this paper to examine the ductility of part-through asymmetric cracks in plates by reporting the results of some experiments in both asymmetric and symmetric configurations.

## Analytical Background

For two-dimensional problems of materials governed by nonlinear elasticity and deformation-plasticity theory, the $J$ integral is defined as[4]

$$J = \int_\Gamma W \, dy - \vec{T} \cdot \frac{\partial \vec{u}}{\partial x} \, ds \qquad (1)$$

where $\Gamma$ = contour surrounding the crack tip, $\vec{T}$ = traction vector along the contour, $\vec{u}$ = displacement vector on the contour, and $W$ = strain-energy density on the contour. The $x$–$y$ coordinate system is such that the crack is parallel to the $x$ axis. In the following we shall evaluate the $J$ integral from far-field quantities for the symmetric and asymmetric case.

Consider a line-integration contour in a single-edge notched specimen as shown in Figs. 2(a) and (b). Along the vertical segments 12, 34, which are free surfaces, the second term of the integrand vanishes because $\vec{T} = 0$. Along the grips (outer boundaries) the displacement $\vec{u}$ is assumed constant so

G.A. Kardomateas is Assistant Professor, School of Aerospace Engineering, Georgia Institute of Technology, Atlanta, GA 30332-0150.

$$\frac{\partial \vec{u}}{\partial x} = 0 \qquad (2)$$

Thus the second term of the $J$ integral expression vanishes everywhere. For rigid nonhardening plasticity the work $W$ also vanishes except where the shear band cuts the surface. There, it is given in terms of the shear strength $k$ and shear strain $\gamma$ by

$$W = k\gamma \qquad (3)$$

For a relative displacement $u_s$ across a shear band of width $\delta t$,

$$\gamma = \frac{u_s}{\delta t} \qquad (4)$$
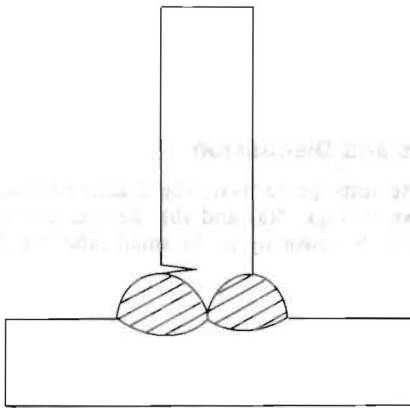


Fig. 1—An asymmetric crack near a weld bead

For the *asymmetric* case, depicted in Fig. 2(a), we have a single shear band at an angle $\theta_s$ from the transverse. For this case, a macromechanical model for crack advance has been developed in Ref. 5 and this will be helpful in defining the quantities needed for evaluating the $J$ integral. As shown in Fig. 3(a), cracking to the new site occurs at an angle $\theta_c$, smaller than $\theta_s$, followed by sliding off. When the process is repeated, the upper surface consists entirely of 'cracked' material, whereas the lower surface consists of a mixture of sheared-off and cracked material. The crack is assumed to grow by an amount $du_c \cos \theta_c$ due to cracking and then by an amount $du_s \cos \theta_s$ due to slipping along the plane, making an angle $\theta_s$ with the transverse. (At the same time the back surface opposite the groove will be drawn in by an amount equal to the slipping one.) The direction of crack growth is denoted by $\theta_f$ [Fig. 2(a)] and is defined from the angles and amounts of slipping and cracking.[5] Therefore, the axial extension is from Fig. 3(a):

$$u_s = \frac{u_a}{\sin \theta_s} \qquad (5)$$

The band thickness is from Fig. 2(a):

$$\delta t = \delta y \cos (\theta_s - \theta_f) \qquad (6)$$

Using the above, we obtain

$$J_{asym} = W\delta y = \frac{k u_a}{\sin \theta_s \cos (\theta_s - \theta_f)} \qquad (7)$$

For the *symmetric* case [Fig. 3(b)], the crack in both its upper and lower flanks is assumed to grow by an amount $dx_c$ due to cracking along the transverse direction, and then by an amount $dx_s$ due to slipping along the plane making an angle $\theta_s$ with the transverse. The axial extension in this case is found from Fig. 3(b),
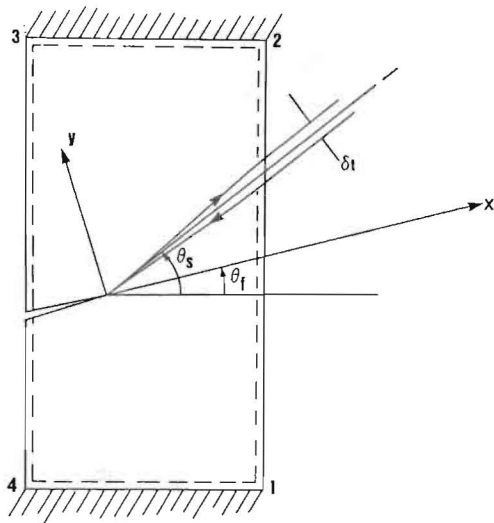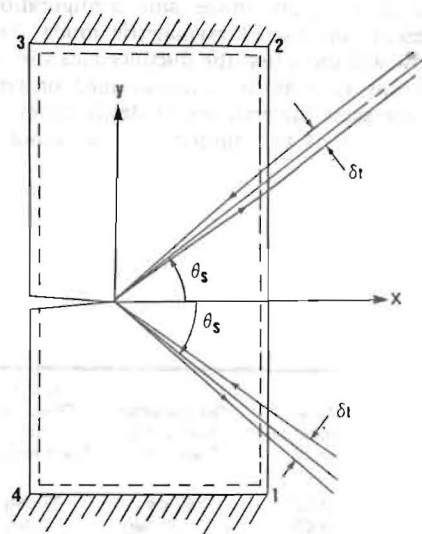


(a)  (b)

Fig. 2—Contour for the evaluation of the $J$ integral; (a) for the asymmetric case and (b) for the symmetric case

$$u_a = 2u_s \sin \theta_s \qquad (8)$$

Now the thickness of each band is from Fig. 2(b),

$$\delta t = \delta y \cos \theta_s \qquad (9)$$

Thus, by substituting in eq (1),

$$J_{sym} = 2W \delta y = \frac{2ku_a}{\sin 2\theta_s} \qquad (10)$$

Now having obtained the expressions of the $J$ integral in terms of the axial displacement, we can find expressions for the tearing modulus of Paris et al.[6] in terms of the axial displacement per unit crack advance, $du_a/dc$, which measures the crack-growth ductility. The tearing modulus is defined in terms of the yield or tensile strength $\sigma_0$, the modulus $E$ and the $J$ integral by

$$T = \frac{E}{\sigma_0^2} \frac{dJ}{dc} \qquad (11)$$

Use $\sigma_0 \simeq T.S. \simeq k\sqrt{3}$, to get

$$T_{asym} = \frac{E}{\sqrt{3}\,(T.S.)} \frac{1}{\sin \theta_s \cos (\theta_s - \theta_f)} \frac{du_a}{dc} \qquad (12)$$

and for the symmetric case

$$T_{sym} = \frac{E}{\sqrt{3}\,(T.S.)} \frac{2}{\sin 2\theta_s} \frac{du_a}{dc} \qquad (13)$$

For growth along the shear band in the asymmetric case ($\theta_f = \theta_s$) and for shear band orientations at 45 deg in both cases, the expression for the tearing modulus in the symmetric case has a $\sqrt{2}$ factor over that of the asymmetric case; but for growth along the transverse in the asymmetric case the expressions for the tearing modulus would be the same. The axial displacement per unit crack advance is also related to the crack-opening angle, COA,[1] the two quantities being in general proportional for small crack-opening angles. It should be noted that single-parameter measures of ductile crack propagation, for example, COA, can apply only if they are referred to crack extension in a certain mode and configuration, such as the present constrained asymmetric mode. Test results that follow will show that the ductility measures of other configurations such as the unconstrained or symmetric cases of the same material are modestly different. A complete discussion of this subject can be found in Ref. 1.

## Test Procedure

Tests were performed on plates with part-through cracks of 1018 cold finished steel with mechanical properties derived from tensile tests on 1-in. gage length, 0.25-in. diameter specimens as follows: yield strength 586 MN/m², tensile strength 600 MN/m², hardness 187 Kgf/mm², reduction in area 49 percent. The specimens were machined from 21-in. × 3.5-in. × 0.5-in. plates as shown in Figs. 4(a) and (b). A 45-deg groove was introduced for a third of the net thickness and half plate width in both geometries. In the asymmetric specimens, the asymmetry is introduced with a shoulder; the ratio of the shoulder to net ligament is one to three.

After testing in tensile loading until complete separation (grips displaced in the axial direction), the topographies of the fracture surfaces were plotted using a metallurgical microscope with a traveling stage whose coordinates are recorded with two linear potentiometers. The microscope plots can be used to obtain the geometry of the fracture[1]: lower and upper flank angles $\theta_l$ and $\theta_u$, respectively, displacement vector (magnitude of the axial displacement $u_a$ and orientation of the displacement vector from transverse $\phi$), crack-opening angle, $\omega$, lower and upper flank lengths $\ell_l$, $\ell_u$, respectively.

## Results and Discussion

For the tests performed, the fracture-surface profiles are shown in Figs. 5(a) and (b). Results are summarized in Table 1. Noteworthy is the small (about 6-deg) crack-



(a)



(b)
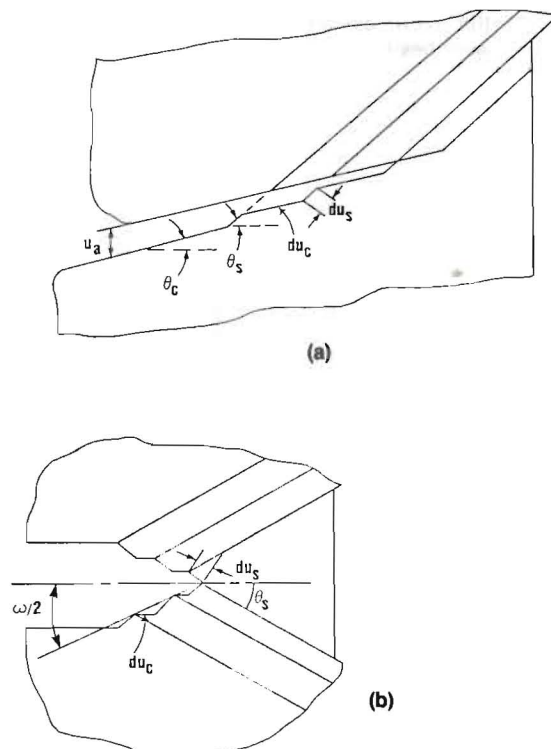
Fig. 3—Macromechanical model of crack advance by slipping and fracture; (a) in the asymmetric case and (b) in the symmetric case

TABLE 1—TEST RESULTS

| | Crack-opening angle, $\omega$ | Growth Displacement $u_a/\ell_0$ | Displacement Vector from Transverse $\phi$ | Crack Direction from Transverse $\theta_f$ |
|---|---|---|---|---|
| Asymmetric | 6 deg | 0.234 | 67 deg | 39 deg |
| Symmetric | 36 deg | 0.470 | ($\simeq$ 90 deg) | 2 deg |

| Tearing Modulus, $T$ [see eqs (12) and (13)] | |
|---|---|
| Asymmetric | 66.3 |
| Symmetric | 187.2 |

opening angle of the asymmetric case as opposed to the large crack-opening angle (about 36 deg) of the symmetric one. The crack-growth ductility, defined in Ref. 1 as the minimum displacement per unit ligament reduction, is about twice the crack-opening angle in the asymmetric case and about the crack-opening angle itself in the

symmetric case. The growth displacement can be found from the fracture-surface profiles. The normalized axial displacement during crack growth, $u_a/\ell_0$, is about two times larger in the symmetric than the asymmetric case. The total displacement vector is at about $\phi = 67$ deg from the transverse indicating a large Mode I component in the local plastic flow; this value is also larger than the one for unconstrained singly grooved tests.[1] The crack direction is itself less than 45 degrees by 6 degrees, indicating the effect of higher triaxiality on one side. While the symmetric cracks were stable, in the asymmetric specimens the crack was only initially stable. In one of the asymmetric specimens, the shear instability was followed by cleavage (identified by the characteristic visual shiny appearance), even at room temperature.

The tearing modulus was found by using eqs (12) and (13) and approximating $du_a/dc \simeq u_a/\ell_0$. We also used a modulus of $E = 207,000$ MN/m$^2$ for the steel and $T.S. = 600$ MN/m$^2$ and assumed shear bands at $\theta_s = 45$ deg. Data for the tearing modulus are shown in Table 1; the value for the symmetric specimen being about three times
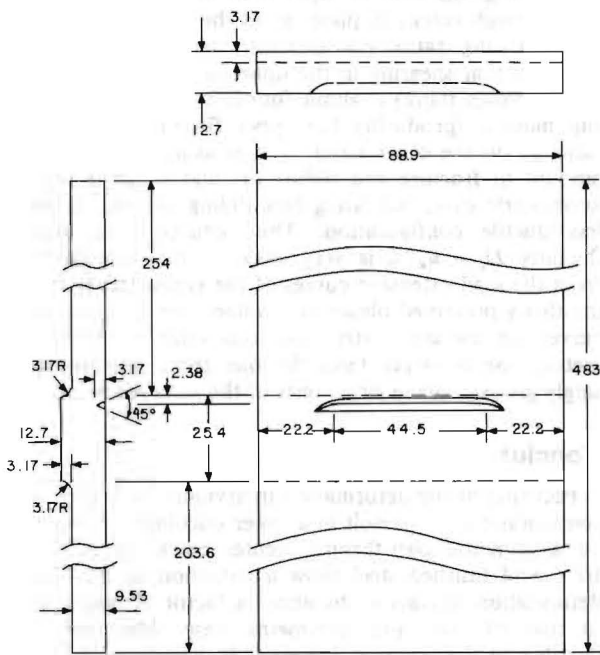


Fig. 4(a)—The asymmetric part-through crack specimen
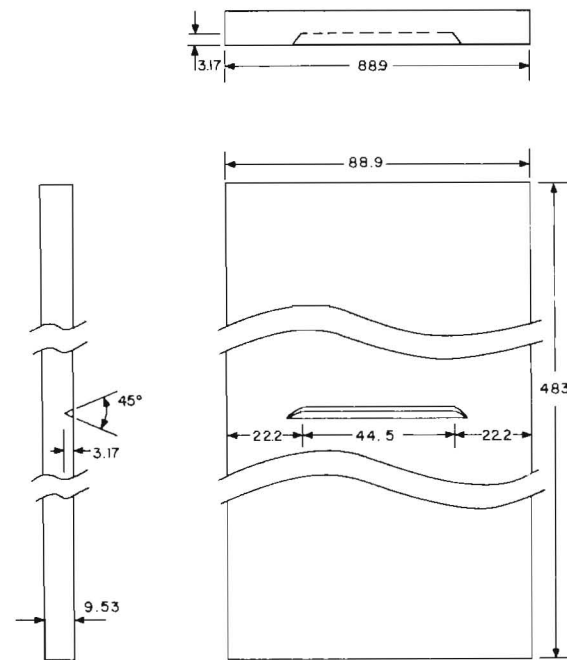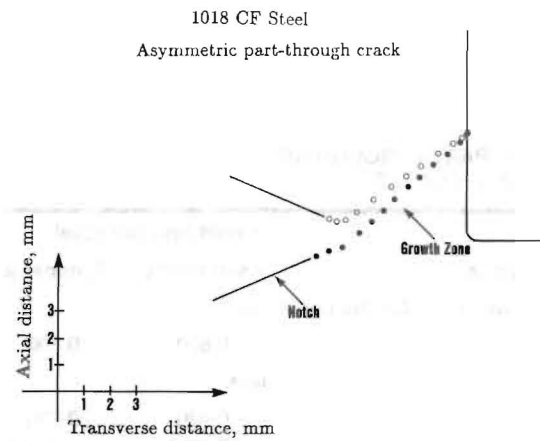




Fig. 5(a)—Fracture surface profile for the asymmetric part-through crack



Fig. 4(b)—The symmetric part-through crack specimen
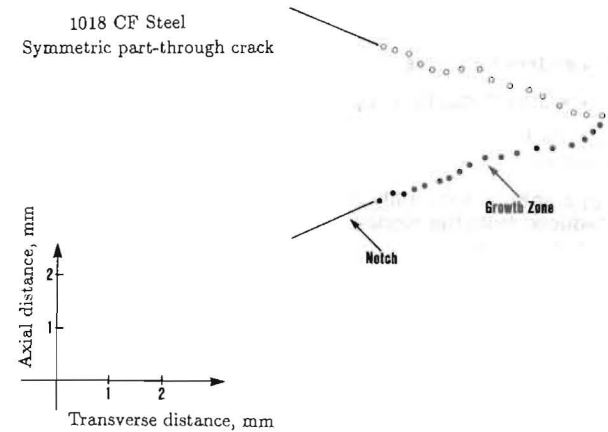


Fig. 5(b)—Fracture surface profile for the symmetric part-through crack

that for the asymmetric one underlines the reduction in crack-growth resistance encountered in the asymmetric case.

To provide a better physical basis for interpreting the test data, the fully plastic crack growth in such asymmetric and symmetric specimens was characterized by the directions and amounts of fracture and slip on three planes.[2] In particular, the model assumes in the general mixed mode I and II case, sliding off along two slip planes and fracture on a third and gives the physical variables (shear and cracking directions, relative amounts of cracking and shearing) in terms of the observable quantities of the macroscopic fracture (flank angles, flank lengths, back angle).

Specifically, assume cycles of sliding off on an upper slip plane at $\theta_{su}$ through a distance $s_u$, then on a lower at $\theta_{sl}$ through $s_l$ and finally fracture at $\theta_c$ over a distance $f$. The limiting Mode I case with two symmetric slip planes corresponds to $\theta_{su} = -\theta_{sl}$, $\theta_f = 0$ deg, $s_u = s_l$, and the limiting Mode II single-slip plane case corresponds to $s_l = 0$. Thus, there are five independent physical variables: the slip and fracture angles, $\theta_{su}$, $\theta_{sl}$, $\theta_c$, and the cracking ratio $\chi = f/s_u$ and the shearing ratio $\xi = s_l/s_u$. Observable quantities that allow solving for the physical variables are

the flank angles, $\theta_l$, $\theta_u$, the flank lengths normalized with the initial ligament, $\ell_u/\ell_0$, $\ell_l/\ell_0$, and the back angle, $\beta_u$, defined as the angle the deformed back surface makes to the load axis. This two slip plane model accounts for the presence of a Mode I component in the asymmetric case. There are five equations that connect the observable quantities with the physical variables and a direct solution can be found[2] for the latter ones. Notice that the observable quantities needed are obtained from the fracture-surface profiles [see Figs. 5(a) and (b)].

Applying this kind of analysis to the test data for the part-through cracks in plates gives the results in Table 2. The shearing ratio $\xi = s_l/s_u$ in the asymmetric case indicates that shearing in the upper slip band $s_u$ (producing the lower flank) is about four times that in the lower slip band $s_l$ (producing the upper flank). The cracking ratio $\chi$, on the other hand, is a measure of the relative amount of fracture and sliding off and is larger for the asymmetric case, indicating less sliding off and hence a less ductile configuration. The deduced crack-growth ductility $D_g = u_a/\ell_0$ is very close to the one obtained from the load-extension curves of the symmetric tests (the instability prevented obtaining a value from load-extension curves for the asymmetric case). Its value for the asymmetric case is larger than the one from unconstrained singly grooved plane strain tests of the same material.[1]

## Conclusion

Focusing of the deformation in asymmetric fully plastic configurations may result in a lower ductility. Experiments on asymmetric part-through center cracks in plates of 1018 cold finished steel show a reduction in the overall deformation to fracture by about a factor of two relative to that of the usual symmetric case. Moreover, the ductility of the asymmetric case is two to three times the corresponding one from unconstrained singly grooved plane-strain asymmetric tests of the same material. The crack-growth resistance is quantified by deriving appropriate expressions for the $J$ integral and the tearing modulus in both the asymmetric and symmetric cases.

TABLE 2—PART-THROUGH ASYMMETRIC AND SYMMETRIC CRACKS

| Alloy | 1018 cold finished steel | |
|---|---|---|
| Observations | Asymmetric | Symmetric |
| Length ratio, $\ell_u/\ell_0$, for the upper flank | | |
| | 0.830 | 0.700 |
| Length ratio, $\ell_l/\ell_0$, for the lower flank | | |
| | 0.930 | 0.700 |
| Upper-flank angle, $\theta_u$ | 36 deg | −16 deg |
| Lower-flank angle, $\theta_l$ | 42 deg | 20 deg |
| Upper-back angle, $\beta_u$ | 15 deg | 16 deg |
| Corresponding slip and fracture parameters | | |
| Lower-slip angle, $\theta_{sl}$ | −19 deg | −34 deg |
| Upper-slip angle, $\theta_{su}$ | 51 deg | 40 deg |
| Cracking angle, $\theta_c$ | 40 deg | 0.2 deg |
| Cracking ratio, $\chi$ | 3.64 | 1.02 |
| Shearing ratio, $\xi$ | 0.27 | 0.92 |
| Dependent Variables | | |
| Crack-growth ductility, $D_g = u_a/\ell_0$ | | |
| Deduced | 0.234 | 0.456 |
| Load-ext | — | 0.470 |
| Apparent crack ductility on upper flank, $D_{AC,u}$ (deduced from the model) | | |
| | 0.041 | 0.472 |
| Apparent crack ductility on lower flank, $D_{AC,l}$ (deduced from the model) | | |
| | 0.213 | 0.495 |
| Upper shear band strain, $\gamma_u$ (deduced) | | |
| | 1.015 | 0.649 |
| Lower shear band strain, $\gamma_l$ (deduced) | | |
| | −0.068 | −0.601 |

### References

1. Kardomateas, G.A. and McClintock, F.A., "Tests and Interpretation of Mixed Mode I and II Fully Plastic Crack Growth from Simulated Weld Defects," Int. J. of Frac., 35, 103-124 (1987).
2. Kardomateas, G.A. and McClintock, F.A., "Shear Band Characterization of Mixed Mode I and II Fully Plastic Crack Growth," Int. J. of Fract., 40, 1-12 (1989).
3. McClintock, F.A., "Plasticity Aspects of Fracture," Fracture, ed. H. Liebowitz, Academic Press, New York, 3, 47-225 (1971).
4. Rice, J.R., "A Path Independent Integral and the Approximate Analysis of Strain Concentration by Notches and Cracks," J. Appl. Mech., 379-386 (1968).
5. Kardomateas, G.A., "Macro-Mechanical Analysis for Symmetric and Asymmetric Fully Plastic Crack Growth," J. Eng. Mat. and Tech. (ASME), 108, 285-289 (1986).
6. Paris, P.C., Tada, H., Ernst, H. and Zahoor, A., "The Theory of Instability of the Tearing Mode of Elastic-Plastic Crack Growth," Elastic-Plastic Fracture, ASTM STP 668, 5-36 (1979).